Available online at www.sciencedirect.com

SCIENCE DIRECT®

Polymer 46 (2005) 9955–9964

polymer

www.elsevier.com/locate/polymer

A theoretical investigation on the electronic and optical properties of π-conjugated copolymers with an efficient electron-accepting unit bithieno[3,2-*b*:2′3′-*e*]pyridine

Li Yang[a], Ji-Kang Feng[a,b,*], Yi Liao[b,c], Ai-Min Ren[a]

[a]*State Key Laboratory of Theoretical and Computational Chemistry, Institute of Theoretical Chemistry, Jilin University, Changchun 130023, People's Republic of China*

[b]*College of Chemistry, Jilin University, Changchun 130023, People's Republic of China*

[c]*Institute of Functional Material Chemistry, Faculty of Chemistry, Northeast Normal University, Changchun 130024, People's Republic of China*

Received 4 November 2004; received in revised form 31 May 2005; accepted 19 July 2005

Abstract

One of the drawbacks for light-emitting diodes based on polyfluorene and derivatives (PFs) is the injection of electrons from the cathode due to the low electron affinity (EA) of most derivatives. Substitution by electron-accepting charge carriers on the conjugated polymer's backbone produces a remarkable influence on its electronic and optical properties. In this contribution, we apply quantum-chemical techniques to investigate a family of π-conjugated polymers poly(fluorene-*alt-co*-bithieno[3,2-*b*:2′3′-*e*]pyridine) (PFBTP) and poly(indenofluorene-*alt-co*-bithieno[3,2-*b*:2′3′-*e*]pyridine) (PIFBTP). The electronic properties of the neutral molecules, HOMO–LUMO gaps (Δ_{H-L}), in addition to the positive and negative ions, are studied using B3LYP functional. The lowest excitation energies (E_g) and the maximal absorption wavelength (λ_{abs}) of PFBTP and PIFBTP are studied employing the time dependent density functional theory (TD-DFT) and semiempirical method ZINDO. The IP, EA and λ_{abs} of the polymers were also obtained by extrapolating those of the oligomers to the inverse chain length equal to zero ($1/n=0$). Especially, the influence of the presence of bithieno[3,2-*b*:2′3′-*e*]pyridine (BTP) groups on to the fluorene or indenofluorene moieties on the electron-accepting and -transporting is emphasized. As shown the BTP is a good electron-accepting moiety for electronic materials due to the presence of the three electron negative heteroatoms. For both PFBTP and PIFBTP, the LUMOs are significantly lower about 0.6 eV than that of their corresponding polyfluorene (PF), which results in the increasing of EAs by about 0.6 eV than PF, indicating that the bithieonpyridine units have significantly improved the electron-accepting properties of the copolymers. These cause the band gap narrower and the maximal absorption red-shifted comparing with PF.

Keywords: Fluorene; DFT; Extrapolation

1. Introduction

In recent years, a great deal of interest has been focused on the synthesis of novel π-conjugated polymers, because of their intriguing properties such as electrical conductivity [1], electroluminescence [2], third-order non-linear optical properties [3] and chemical sensing [4,5]. One major problem with organic polymers for such applications is that they are usually much better at accepting and transporting holes than electrons. This is a limiting factor in the development of light-emitting diodes (LEDs) as obtaining balanced charge injection and transport is necessary for obtaining high device efficiencies. Many ways have been used to modulate the ionization potential (IP), electron affinity (EA), and band gaps of polyfluorenes derivatives including conjugation length control, as well as the introduction of electron-donating or -accepting groups to the parent chromophore [6–9].

Quantum-chemical calculations for the better understanding of the electronic properties of polyaromatic oligomers and polymers have contributed a lot to rationalize

---

[*] Corresponding author. Address: State Key Laboratory of Theoretical and Computational Chemistry, Institute of Theoretical Chemistry, Jilin University, Changchun 130023, People's Republic of China. Fax: +86 431 8945942.

E-mail address: jikang@yahoo.com (J.-K. Feng).

0032-3861/$ - see front matter © 2005 Elsevier Ltd. All rights reserved.
doi:10.1016/j.polymer.2005.07.058

the properties of known polymers [10–17] and to predict those of yet unknown ones [18]. Semiempirical methods are known to yield satisfactory geometries and can provide a good insight in the electronic structure of large systems [19–23]. In the present work we have shown that scaled semiempirical energy gaps are in good agreement with reported experimental results. Correlation effects can be very important for the study of electronic structure of molecules and should be taken into account particularly when one is interested in the evaluation of the energy gap. In this sense, density functional theory (DFT), due to its feature of including the electronic correlation in a computationally efficient manner, can be used in larger molecular systems [19–21,24–28]. In its formalism, the ionization potential and electron affinity are well-defined properties than can be calculated.

In this paper, bithieno[3,2-*b*:2′3′-*e*]pyridine (BTP) [29] served for a novel electron-accepting monomer and the copolymer with fluorene and indenofluorene have been investigated. To test its electronic properties, polymer fluorene, which has high LUMO energy levels and so are poor electron acceptors, has been employed to compare with them. Here, we explore the ground and low-lying excited states of polymers poly(fluorene-*alt-co*-bithieno[3,2-*b*:2′3′-*e*]pyridine) (PFBTP) and poly(indenofluorene-*alt-co*-bithieno[3,2-*b*:2′3′-*e*]pyridine) (PIFBTP) [29] by theoretical studies. The majority of the studies on polymers using quantum-chemistry methods consider, in fact, oligomers. The general strategy is the simulation of a number of oligomers of increasing length such that the properties of the polymers can be inferred by extrapolating the results [20,24,30–38]. A distinct advantage of this approach is that it can provide the convergence behavior of the structural and electronic properties of oligomers. However, the computational cost increases rapidly from monomer to oligomer, which prevents treatment of these systems using high level of theory. We employ density functional theory (DFT) methods for the ground-state electronic structures, and well-established semiempirical method ZINDO and time-dependent DFT (TDDFT) for optical properties. We were particularly interested in exploring the potential of bithieno[3,2-*b*:2′3′-*e*]pyridines (BTP) as electron-accepting moieties for electronic materials through exploring and comparing the energies of HOMO and LUMO and the variation of IP and EA of polymers poly(fluorene-alt-co-bithieno[3,2-*b*:2′3′-*e*]pyridine) (PFBTP) and poly(indenofluorene-*alt-co*-bithieno[3,2-*b*:2′3′-*e*]pyridine) (PIFBTP) with polyfluorene (PF) [38]. We were similarly interested in understanding whether and how the properties of BTP would modulate the optical characters. On the other hand, we wanted to show the potential of a quantum mechanical modeling based on DFT, in the evaluation of ground and excited state properties by comparison to the available experimental data.

2. Computational details

Calculations on the electronic ground state of oligomers were carried out using density functional theory (DFT), B3LYP/6-31G*. The transition energies will be calculated at the ground-state geometries using ZINDO and TD-DFT/B3LYP calculations, respectively, and the results are compared with the available experimental data. We employed the linear extrapolation technique in this research. The linearity between the calculated IPs, EAs, energy gaps, maximal absorption wavelengths of the oligomers and the reciprocal chain length is excellent for both series of oligomers. The excited geometries were optimized by ab initio CIS/6-31G* [39]. Based on the excited geometries, the emission spectra of part of the molecules are investigated. All calculations on these oligomers studied in this work have been performed on the SGI origin 2000 server using Gaussian 03 program package [40].

3. Results and discussion

3.1. Ground structural properties

The sketch map of the structures for $(FBTP)_n$ and $(IFBTP)_n$ is depicted in Fig. 1 and the optimized structures of $(FBTP)_4$ and $(IFBTP)_4$ from calculations by DFT//B3LYP/6-31G* are given in Fig. 2. The investigated polymer $(FBTP)_n$ and $(IFBTP)_n$ correspond to copolymers P1 and P2 in literature [29], respectively, and the main difference is that the ones under study substitute 9,9-dihexyl with methyl in fluorine rings for the sake of reducing the time of calculation. In fact, it has been proved that the presence of alkyl groups at 9-positions does not significantly affect the equilibrium geometries and thus the electronic and optical properties [41,42]. In particular, we compare the two systems under study with pristine polyfluorene calculated by our groups [38] recently to gain a deeper insight into the impact of bithieno[3,2-*b*:2′3′-*e*]pyridine (BTP) units on the electronic and optical properties.

The results of the optimized structures for the copolymeric molecules of the $(FBTP)_n$ and $(IFBTP)_n$ ($n=1$–4) show that they have the similar conformations and the bond lengths and bond angles do not suffer appreciable variation with the oligomer size in the serial $(FBTP)_n$, as well as $(IFBTP)_n$. And it suggests that we can describe the basic structures of the polymers as their oligomers. Because the dihedral angle between two phenyl rings in fluorene and indenofluorene segments of both series of oligomers is fixed by ring bridged-atoms which tend to keep their normal tetrahedral angles in their ring linkage to keep their quasi planar conformation, they are no more than 1°. The biggest dihedral angles are the inter-ring dihedral angles between the adjacent BTP and fluorine or indenofluorene rings in $(FBTP)_n$ and $(IFBTP)_n$. The optimized dihedral angles

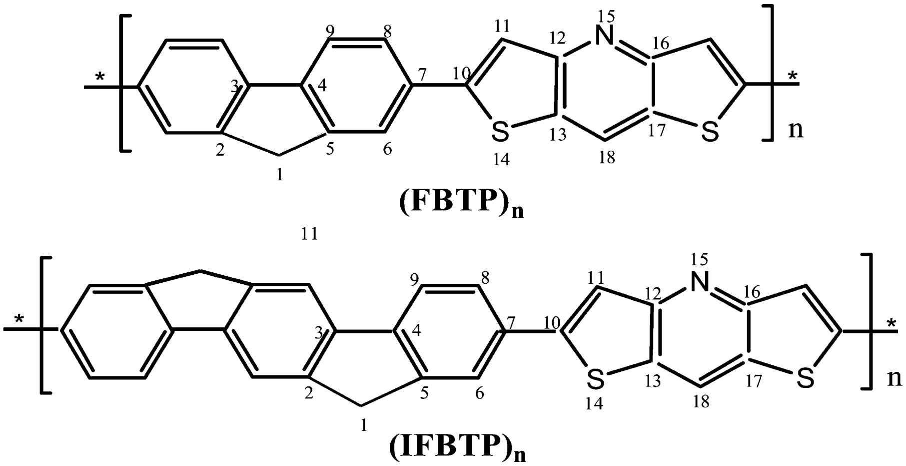

Fig. 1. Chemical structure of $(FBTP)_n$ and $(IFBTP)_n$.

between the subunits of these oligomers are summarized in Table 1, as well as the inter-ring distances.

We found that the consecutive units of an oligomer have similar inter-ring dihedral angles, which average in the oligomers around 25° in both series, which is less twisted than the case in $(F)_n(\sim 36°)$ [38]. This indicates that the good π-conjugated structure of bithieno[3,2-*b*:2′3′-*e*]pyridines improve the whole polymer's coplanarity compared with pristine polyfluorene. Furthermore, as it can be seen from Fig. 2, the $(IFBTP)_4$ has better planar conformation than $(FBTP)_n$, which attributed to an increase of polymer chain planarity and effective conjugation length upon substitution of indenofluorene for fluorene.

3.2. Front molecular orbitals

It will be useful to examine the highest occupied orbitals (HOMO) and the lowest virtual orbitals (LUMO) for these oligomers and polymers because the relative ordering of the occupied and virtual orbitals provides a reasonable qualitative indication of the excitation properties [43] and of the ability of electron or hole transport. Because the first dipole-allowed electron transitions, as well as the strongest electron transitions with largest oscillator strength correspond almost exclusively to the promotion of an electron from HOMO to LUMO, we have plotted the contour plots of HOMO and LUMO orbitals of $(FBTP)_n$ ($n=1$–4) and $(IFBTP)_n$ ($n=1$–4) by B3LYP/6-31G* in Fig. 3.

As shown in Fig. 3, in general, the electronic cloud distributing in $(FBTP)_n$ is similar to that in $(IFBTP)_n$ and all the frontier orbitals spread over the whole π-conjugated backbone, although the largest contributions come from the different parts of the chromophores. There is anti-bonding between the bridge atoms of inter-ring and there is bonding between the bridge carbon atom and its conjoint atoms of intra-ring in the HOMO. On the contrary, there are bonding in the bridge single bond of inter-ring and the antibonding between the bridge atom and its neighbour of intra-ring in the LUMO. In general, the HOMO possesses an antibonding character between the subunits. This may explain the non-planarity observed for these oligomers in their ground states. On the other hand, the LUMO of all the oligomers generally shows a bonding character between the two adjacent subunits. This implies that the singlet excited state involving mainly the promotion of an electron from the HOMO to the LUMO should be more planar. For LUMO in both $(FBTP)_n$ and $(IFBTP)_n$, the electronic clouds transfer to fluorene or indenofluorene ring from BTP units and mainly localized on the bridge bond. For the polymers, this implies the BTP moiety serves as electron-accepting moieties for electronic materials and is anticipated to have high electron affinity due to the presence of three electronegative heteroatoms.

In experiment, the HOMO and LUMO energies were calculated from one empirical formula proposed by Brédas et al., based on the onset of the oxidation and reduction

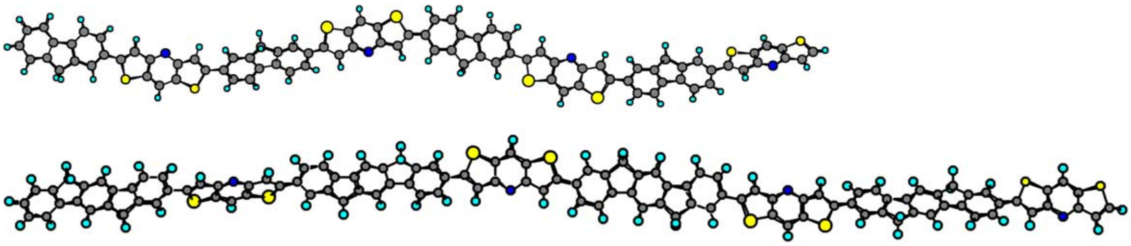

Fig. 2. Optimized structures by DFT//B3LYP/6-31G* for $(FBTP)_4$ (up) and $(IFBTP)_4$ (down).

Table 1
Selected important dihedral angles and inter-ring distances of $(FBTP)_n$ and $(IFBTP)_n$ ($n=1$–4) obtained by B3LYP/6-31G* calculations

Oligomer		F–B	B–F	F–B	B–F	F–B	B–F	F–B
$(FBTP)_n$								
$n=1$	Φ (deg)	25.6						
	r (Å)	1.466						
$n=2$	Φ (deg)	25.5	25.2	25.2				
	r (Å)	1.466	1.466	1.466				
$n=3$	Φ (deg)	26.1	24.6	25.3	24.9	23.8		
	r (Å)	1.466	1.466	1.466	1.466	1.466		
$n=4$	Φ (deg)	25.6	25.5	24.9	24.4	24.4	24.4	24.9
	r (Å)	1.466	1.466	1.466	1.466	1.466	1.466	1.466
Oligomer		I–B	B–I	I–B	B–I	I–B	B–I	I–B
$(IFBTP)_n$								
$n=1$	Φ (deg)	25.1						
	r (Å)	1.466						
$n=2$	Φ (deg)	25.0	25.0	25.1				
	r (Å)	1.466	1.466	1.466				
$n=3$	Φ (deg)	25.4	24.5	24.6	24.9	24.7		
	r (Å)	1.466	1.466	1.466	1.466	1.466		
$n=4$	Φ (deg)	25.4	24.8	24.3	23.8	23.9	24.2	25.5
	r (Å)	1.466	1.466	1.466	1.466	1.466	1.466	1.466

Note: F, means the fluorene ring; I, is the indenofluorene ring and B, is the bithieno[3,2-*b*:2′3′-*e*]pyridine ring in every molecule.

peaks measured by cyclic voltammetry, assuming the absolute energy level of ferrocene/ferrocenium to be 4.8 eV below vacuum [11]. Whereas the HOMO and LUMO energies can be calculated accurately by density functional theory (DFT) in this study. Fig. 4 describes the evolution of the B3LYP/6-31G* calculated highest occupied molecular orbital (HOMO) and lowest unoccupied molecular orbital (LUMO) energies as a function of the inverse number of monomer units in $(FBTP)_n$ and $(IFBTP)_n$. For the sake of comparison, the frontier energy levels of PF are also listed in Fig. 4.

As is usual in π-conjugated systems, the energy of the frontier electronic levels evolves linearly with inverse chain length in both systems [44]. Similar energies are obtained for the LUMO of the $(FBTP)_n$ and $(IFBTP)_n$ oligomers. The introduction of BTP units lowers significantly the LUMO of the longest oligofluorene chains by some 0.6 eV. It can be deduced that the high electron affinity of BTP chains should thus ensure efficient electron injection and low charge trapping in devices. Turning to the evolution of the HOMO levels, we find that while similar energies are calculated for the three systems, the HOMOs of PIFBTP are destabilized by less than 0.2 eV with respective to PFBTP chains due to the substitution of indenofluorene by fluorene. This reduction in the HOMO–LUMO gap observed when going from PF to PFBTP and to PIFBTP will impact the optical properties of the chains. This result of Fig. 4 can be easily rationalized by analyzing the nature of the frontier electronic levels. In PFBTP and PIFBTP, as well as PF, the HOMO remains delocalized along the conjugated backbone; the shapes of the LUMOs become drastically different, being localized on the BTP units in the copolymers and delocalized in the fluorene chains. This is rationalized by the fact that the energy separation between the LUMO of PFBTP and PIFBTP is smaller than that of PF. In contrast, the separation between the corresponding HOMO levels is smaller.

3.3. HOMO–LUMO gaps and the lowest excitation energies

There are two theoretical approaches for evaluating the energy gap in this paper. One way is based on the ground-state properties, from which the energy gap is estimated from the energy difference between the highest occupied molecular orbital (HOMO) and the lowest unoccupied molecular orbital (LUMO), when $n=\infty$, termed the HOMO–LUMO gaps ($\Delta_{\text{H–L}}s$). The implicit assumption underlying this approximation is that the lowest singlet excited state can be described by only one singly excited configuration in which an electron is promoted from HOMO to LUMO. In addition, the orbital energy difference between HOMO and LUMO is still an approximate estimate to the transition energy since the transition energy also contains significant contributions from some two-electron integrals. The real situation in experiment is that an accurate description of the lowest singlet excited state requires a linear combination of a number of excited configurations, although the one mentioned above often plays a dominant role. The TDDFT, which has been used to study systems of increasing complexity due to its relatively low computational cost and also to include in its formalism the electron correlation effects, is also employed to extrapolate energy gap of polymers from the calculated first dipole-allowed excitation energy of their oligomers.

Here, the HOMO–LUMO gaps ($\Delta_{\text{H–L}}$s) and lowest singlet excited energies (E_g) obtained by TDDFT and

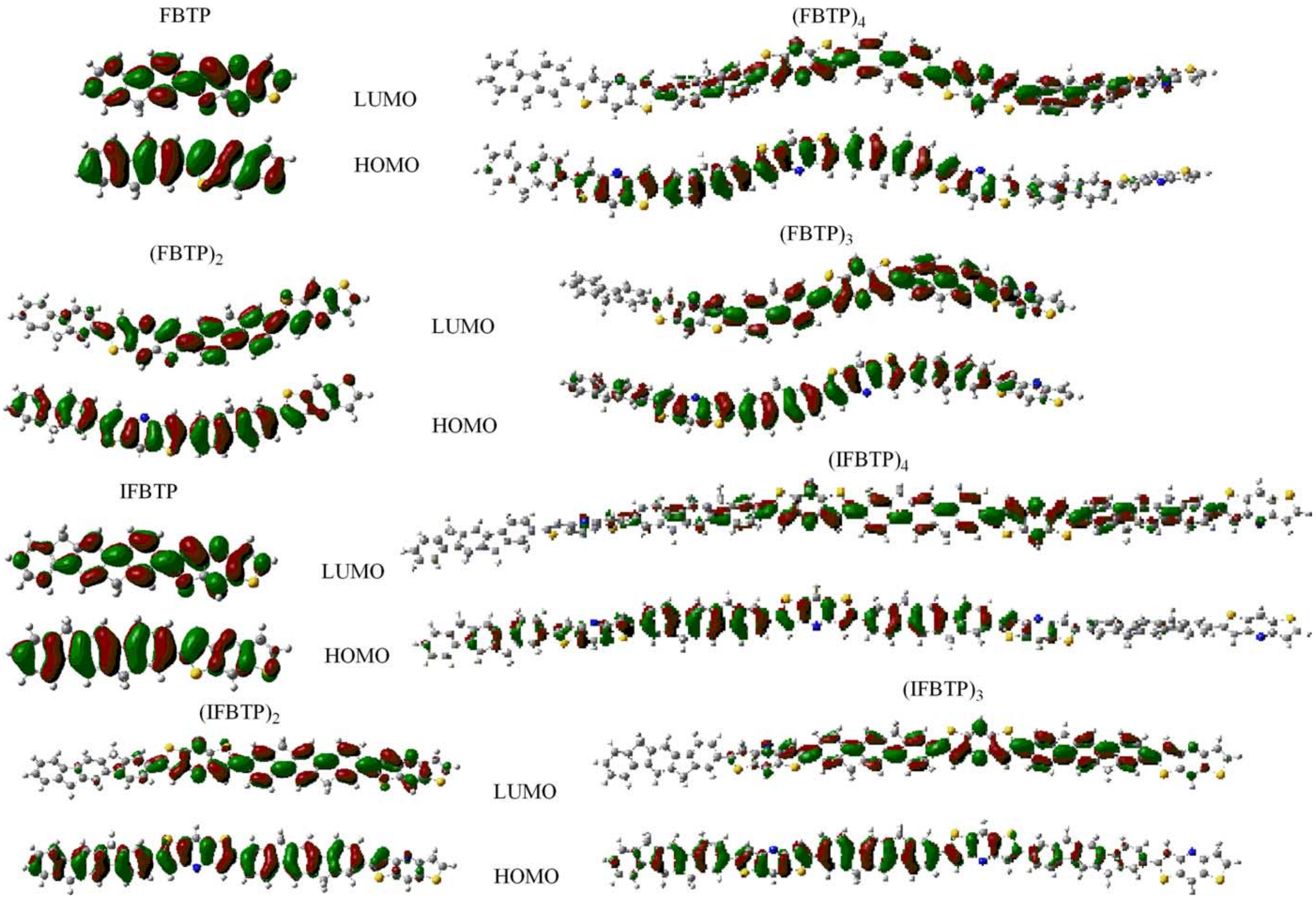

Fig. 3. The HOMO and LUMO orbitals of (FBTP)$_n$ and (IFBTP)$_n$ ($n = 1$–4) by B3LYP/6-31G*.

ZINDO are all listed in Table 2 and the relationships between the calculated $\Delta_{\mathrm{H-L}}$ and the E_g and the inverse chain length are plotted in Fig. 5. There is a good linear relation between the energy gaps by all methods and the inverse chain length. Interesting, the $\Delta_{\mathrm{H-L}}$ presented in Table 2 yield a good agreement with the experimental data compared to E_g in both series in this study, with the discrepancies of 0.11 and 0.02 eV for (FBTP)$_n$ and (IFBTP)$_n$, respectively. TDDFT systematically underestimated the energy gap by 0.18–0.23 eV comparing to the experimental value from the edge of the electronic band due to (1) the limitation of the current approximate exchange-correlation

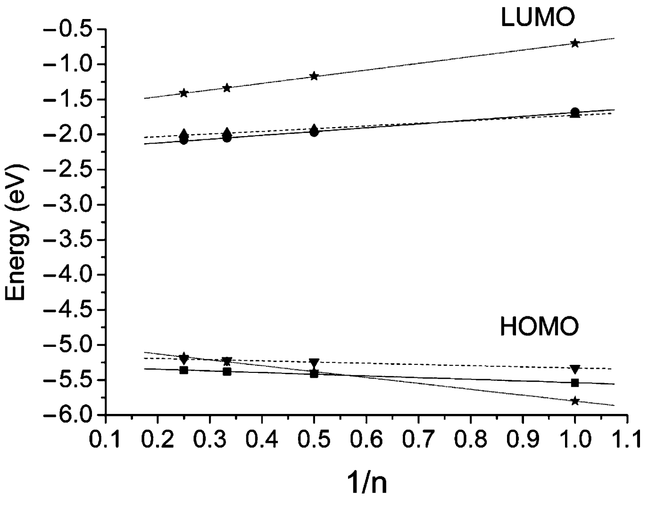

Fig. 4. B3LYP/6-31G* calculated HOMO and LUMO energies of (FBTP)$_n$ (solid lines), (IFBTP)$_n$ (dash dot lines) and (F)$_n$ [38] (short dot) oligomers as a function of the inverse number of monomer units.

Table 2
The HOMO–LUMO gaps (eV) by DFT and the lowest excitation energies (eV) by TDDFT and ZINDO in oligomers of (FBTP)$_n$ and (IFBTP)$_n$

Oligomer	TD-DFT	ZINDO	$\Delta_{\mathrm{H-L}}$
(FBTP)$_n$			
$n = 1$	3.62	3.59	3.87
$n = 2$	3.12	3.36	3.44
$n = 3$	3.03	3.32	3.33
$n = 4$	2.98	3.29	3.28
$n = \infty$	2.79	3.20	3.08
Expl.	2.97		
(IFBTP)$_n$			
$n = 1$	3.36	3.49	3.61
$n = 2$	3.01	3.35	3.31
$n = 3$	2.93	3.31	3.23
$n = 4$	2.91	3.28	3.20
$E_g(n = \infty)$	2.79	3.24	3.04
Expl.	3.02		

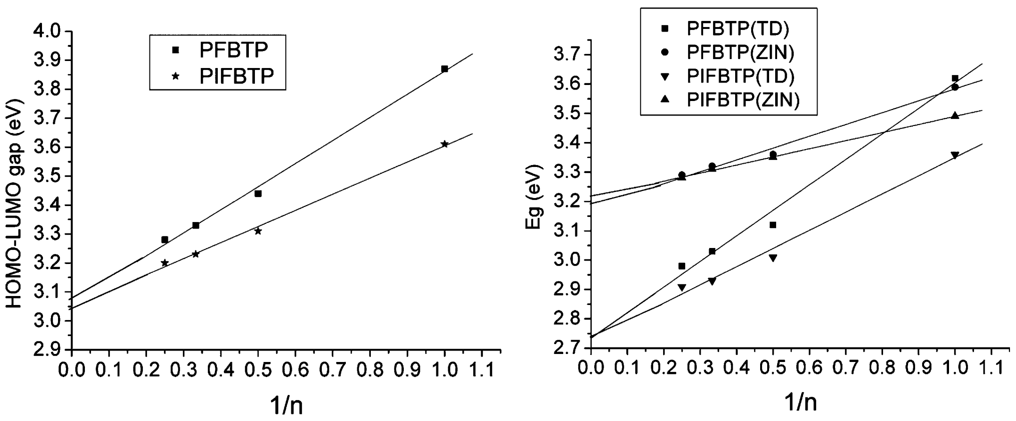

Fig. 5. The HOMO–LUMO gaps (left) by B3LYP and the lowest excitation energies E_g (right) by TD-DFT and ZINDO as a function of reciprocal chain length n in oligomers of $(FBTP)_n$ and $(IFBTP)_n$.

functionals in correctly describing the exchange-correlation potential in the asymptotic region [45–48]; (2) theoretical predictions are made for the isolated gas-phase chains, while experimental band gaps are usually measured in the condensed phase. Additionally, it should be borne in mind that solid-state effects (like polarization effects and intermolecular packing forces) have been neglected in the calculations. The latter can be expected to result in a decreased inter-ring twist and consequently a reduced gap in a thin film compared to an isolated molecule as considered in the calculations [49–51]. In contrast, ZINDO then overestimated the energy gaps around 0.23 and 0.22 eV, respectively.

Moreover, we are interested in the relative excitation energies of the oligomers of the two copolymers to pristine polyfluorene. The band gaps obtained by TD-DFT, ZINDO and HOMO–LUMO gaps are 3.01, 3.24 and 3.42 eV for PF [38], respectively, which are all higher than that of PFBTP with the same corresponding methods of 2.79, 3.20 and 3.08 eV and that of PIFBTP with the values of 2.79, 3.24 and 3.04 eV. On all accounts, the results of each method indicate the same conclusion that the increasing of the conjugation in the backbone narrowed its band gap and vice versa.

3.4. Ionization potentials and electron affinities

As mentioned in the introduction, efficient injection and transport of both holes and electrons are important parameters for the rational design of optimized light-emitting diodes. Ionization potentials (IPs) and electron affinities (EAs) are used to estimate the energy barrier for the injection of both holes and electrons into the polymer. Table 3 contains the ionization potentials (IPs), electron affinities (EAs), both vertical (v; at the geometry of the neutral molecule) and adiabatic (a; optimized structure for both the neutral and charged molecule), and extraction potentials (HEP and EEP for the hole and electron, respectively) that refer to the geometry of the ions [52–54]. The IPs, EAs, HEPs and EEPs are obtained as functions of reciprocal chain length for the oligomers studies, with assumed linear extrapolation to infinite chain length. For PFBTP and PIFBTP, the energy required to create a hole in the polymer is ∼5.6 and ∼5.4 eV, respectively, which are nearly equal to that of PF (5.5 eV) [38], suggesting the ability to create a hole in PFBTP and PIFBTP is comparative to PF as expectation of the energy of HOMO. While the extraction of an electron from the anion requires both nearly 1.8 eV for PFBTP and PIFBTP, which are higher by about 0.6 eV than the corresponding PF (∼1.2 eV) [38], indicating the electron-accepting properties have been improved greatly in PFBTP and PIFBTP due to the introduction of a good electron-accepting moiety bithieno[3,2-*b*:2′3′-*e*]pyridine (BTP), which consists with the estimation of the energy of LUMO.

3.5. Absorption spectra

The TDDFT//B3LYP/6-31G* and ZINDO have been used on the basis of the optimized geometry to obtain the nature and the energy of the singlet–singlet electronic transitions of all the oligomers in all series under study. Here, we list the transition energies, oscillator strengths, configurations and transition dipole moments obtained by TDDFT and ZINDO calculations for the most relevant first three singlet excited states in each oligomer of $(FBTP)_n$ and $(IFBTP)_n$ in Tables 4 and 5. As shown in Tables 4 and 5, all electronic transitions are of the $\pi\pi^*$ type and involve both subunits of the molecule. In other words, no localized electronic transitions are calculated among the first three singlet–singlet transitions. Both methods show that excitation to the S_1 state corresponds almost exclusively to the promotion of an electron from the HOMO to the LUMO. The oscillator strength (*f*) and the transition dipole moment along the long axis of the molecule (χ) of the $S_0 \rightarrow S_1$ electronic transition are large in each oligomer. Considering the fact that the oscillator strength is proportional to the square of the transition moment, it is reasonable that the $S_0 \rightarrow S_1$ transition show a large *f* value.

Table 3
Ionization potentials, electron affinities and extraction potentials for each molecular (in eV) by B3LYP/6-31G*

Oligomer	IP(v)	IP(a)	HEP	EA(v)	EA(a)	EEP
$(\mathrm{FBTP})_n$						
$n=1$	6.81	6.65	6.55	0.50	0.60	0.81
$n=2$	6.28	6.18	6.11	1.17	1.20	1.38
$n=3$	6.05	6.00	5.92	1.43	1.42	1.59
$n=4$	5.92	5.88	5.82	1.58	1.55	1.71
$n=\infty$	5.65	5.65	5.60	1.85	1.82	1.89
$(\mathrm{IFBTP})_n$						
$n=1$	6.46	6.34	6.24	0.66	0.74	0.94
$n=2$	6.00	5.93	5.86	1.22	1.24	1.39
$n=3$	5.80	5.75	5.70	1.45	1.43	1.57
$n=4$	5.68	5.65	5.61	1.57	1.53	1.67
$n=\infty$	5.47	5.45	5.43	1.84	1.79	1.89

The suffixes (v) and (a), respectively, indicate vertical and adiabatic values.

Furthermore, the oscillator strength coupling the lowest CT π–π^* singlet excited state to the ground state increase strongly when going from an isolated molecule to a molecular group. The oscillator strength associated with the S_1 state increases by about one order of magnitude upon adding one repeated unit to the monomers in both series.

Obviously, the strongest absorption peaks are all assigned to $\pi\pi^*$ electronic transition character arising exclusively from $S_0 \rightarrow S_1$ electronic transition mainly composed by HOMO→LUMO transition. Since the first allowed transitions are also the absorption maximum, they have the same variation trend, which we would not say more than is needed. In fact, there are similar characters and variation trends in $(\mathrm{FBTP})_n$ as in the cases of $(\mathrm{IFBTP})_n$.

It is noteworthy that with the conjugation lengths increasing, the absorption wavelengths increase progressively as in the case of the oscillator strengths of $S_0 \rightarrow S_1$ electronic transition. Many investigations show that TDDFT is a good predictive tool for absorption spectra of molecules. However, this method has defects to study extended systems. Because it is not infrequent that the optical properties reach saturation already for quite short chain length, whereas the orbital energies still continue to change for longer oligomers. It is known, the exchange-correlation (XC) functionals must decrease with increasing chain length (this trend of variation is in line with the expectation that in more extended systems the electronic repulsion is smaller) [55,56]. However, because the atomic structures of the molecules are alike and are calculated with the same methods and basis sets, the results can still reflect some variation trend. The results presented in Tables 4 and 5 are consistent with the experimental observations that: (i) Both series of PFBTP and PIFBTP have longer maximal absorption wavelength than PF (391 nm by TDDFT) [38] as experiment exhibited, due to the good conjugated backbone by the introduction of electron-accepting group BTP; (ii) the maximal absorption peaks in PIFBTP exhibit bathochrome compared with PFBTP due to the substitution of fluorene by indenofluorene.

3.6. The properties of excited structures and the emission spectra

Because the calculation of excited-state properties typically requires significantly more computational effort than is needed for the ground states and dramatically constrains by the size of the molecules, we only optimize the monomers of the both series under study by CIS/3-21G*. Interestingly, the main characters of the front orbitals by HF/3-21G* are same to that by B3LYP/6-31G*. We take IFBTP as an example and compare the excited structure (S_1) by CIS/3-21G* with its ground structure (S_0) by HF/3-21G* in Fig. 6. As shown, some of the bond lengths lengthened, but some shortened. We can predict the differences of the bond lengths between the ground (S_0) and singlet excited state (S_1) from MO nodal patterns. Due to the singlet state corresponds to an excitation from the HOMO to the LUMO in all considered oligomers we can explore the bond lengths variation by analyzing the HOMO and LUMO. The HOMO is bonding across r(7,8), r(5,10), r(9,10), r(1,2), r(2,3), r(2′,3′), r(1′,2′), r(10′,9′), r(5′,10′), r(8′,7′), r(6′,7′) and r(13,14) bonds in IFBTP, but the HOMO has nodes in these regions. Therefore, one would expect elongation of these bonds; the data in the figure shows that these bonds are in fact considerably longer in the excited state. The HOMO has a node across the r(2,10), r(2′,10′), r(3,1′), r(8′,9′), r(5′,6′), r(7′,14) and r(12,13) bonds in IFBTP while the LUMO is bonding. The data confirm the anticipated contraction of these bonds.

The bridge bonds between two conjugation segments rotate to some extent. The inter-ring dihedral angles in FBTP and IFBTP reduced from 28.4 and 27.6° to nearly zero degree, respectively. It is obvious that the excited structure has a strong coplanar tendency in both the series, that is, the conjugation is better in the excited structure. This result agrees well with the estimation from the frontier orbital character.

On the optimized excited geometries, the emission spectra of the monomers of PFBTP and PIFBTP are computed by TD-DFT. As in the case of the absorption spectra, the $S_0 \rightarrow S_1$ fluorescence peaks have the strongest

Table 4
Electronic transition data obtained by TDDFT and ZINDO methods for $(FBTP)_n$ ($n=1$–4) at B3LYP/6-31G* optimized geometry

Electronic transitions	TDDFT//B3LYP/6-31G*(d)			ZINDO				
	λ_{abs} (nm)	f	Main configurations	λ_{abs} (nm)	f	Transition dipole moment (D)		
						X	Y	Z
FBTP								
$S_0 \to S_1$	342.68	1.0984	HOMO→LUMO(0.64)	345.0	1.31042	9.79	−0.24	−0.19
$S_0 \to S_2$	325.19	0.0131	HOMO-1→LUMO(0.65)	310.4	0.24083	−3.94	−0.54	−0.20
$S_0 \to S_3$	297.07	0.3845	HOMO→LUMO+1(0.62)	300.6	0.00564	−0.48	−0.35	0.03
$S_0 \to S_4$	285.05	0.0030	HOMO-2→LUMO(0.58) HOMO-1→LUMO+1(0.21)	286.4	0.00506	0.16	−0.53	0.00
$S_0 \to S_5$	284.13	0.0109	HOMO→LUMO+2(0.47) HOMO-4→LUMO(0.37)	273.0	0.00606	0.34	−0.24	0.41
$(FBTP)_2$								
$S_0 \to S_1$	397.99	2.4776	HOMO→LUMO(0.66)	369.2	3.27649	16.02	−0.38	−0.20
$S_0 \to S_2$	366.98	0.2804	HOMO-1→LUMO(0.67)	338.4	0.16945	0.05	3.45	−0.51
$S_0 \to S_3$	352.12	0.0569	HOMO→LUMO+1(0.62)	317.5	0.25994	4.11	−0.59	−0.44
$S_0 \to S_4$	340.77	0.0212	HOMO-2→LUMO(0.60)	303.4	0.14868	3.07	−0.23	0.22
$S_0 \to S_5$	333.48	0.5148	HOMO-3→LUMO(0.47) HOMO-1→LUMO+1(0.42)	296.2	0.00584	−0.46	0.37	−0.07
$(FBTP)_3$								
$S_0 \to S_1$	408.89	3.8500	HOMO→LUMO(0.65)	373.3	5.20878	20.31	−0.02	0.11
$S_0 \to S_2$	378.55	0.0393	HOMO-1→LUMO(0.54) HOMO→LUMO+1(0.30)	353.3	0.10793	−0.18	1.03	−2.64
$S_0 \to S_3$	373.54	0.1923	HOMO→LUMO+1(0.54) HOMO-1→LUMO(0.38)	332.8	0.63902	−5.27	−3.79	−1.70
$S_0 \to S_4$	363.13	0.1865	HOMO-2→LUMO(0.62)	317.8	0.03054	−0.32	−1.02	0.94
$S_0 \to S_5$	360.01	0.8954	HOMO-1→LUMO+2(0.59)	308.0	0.05490	1.89	−0.04	0.01
$(FBTP)_4$								
$S_0 \to S_1$	415.53	5.1884	HOMO→LUMO(0.61)	375.8	6.95574	−23.56	−0.05	−0.12
$S_0 \to S_2$	392.83	0.0255	HOMO-1→LUMO(0.50) HOMO→LUMO+1(0.42)	361.6	0.02828	−0.05	1.29	−0.69
$S_0 \to S_3$	381.17	0.1481	HOMO→LUMO+1(0.49) HOMO-1→LUMO(0.42)	346.7	0.66328	6.22	−0.29	−3.15
$S_0 \to S_4$	375.15	0.6517	HOMO-1→LUMO+1(0.53) HOMO-2→LUMO(0.20)	332.1	0.34598	−2.86	−3.98	0.54
$S_0 \to S_5$	371.61	0.0972	HOMO-2→LUMO(0.62)	319.2	0.17879	−2.92	1.16	1.49
Exp.	415[a]							

[a] The values are measured in thin film.

oscillator intensity in both series and exclusively mainly arise from HOMO→LUMO ππ* excitation. Although there are some discrepancies between the calculated values and the observed data, they have the same trend that the emission peaks increase going from FBTP (371 nm) to IFBTP (394 nm). Most importantly, pure deep strong blue electronluminescence was successfully achieved from the bithieno[3,2-*b*:2′3′-*e*]pyridine-based copolymers [29].

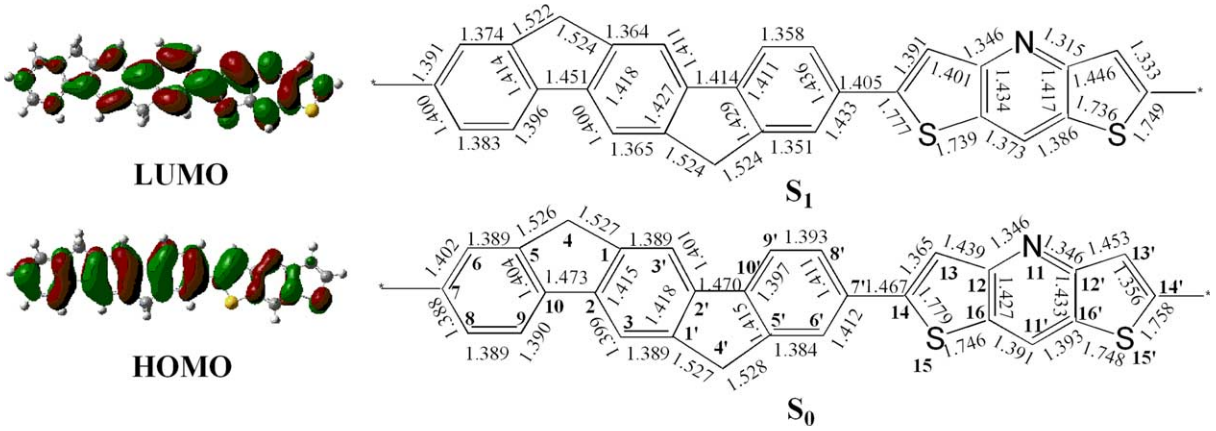

Fig. 6. Comparison of the excited structure (S_1) with the ground geometry (S_0) of IFBTP.

Table 5
Electronic transition data obtained by TDDFT and ZINDO methods for $(IFBTP)_n$ ($n = 1$–4) at B3LYP/6-31G* optimized geometry

Electronic transitions	TDDFT//B3LYP/6-31G*(d)			ZINDO				
	λ_{abs} (nm)	*f*	Main configurations	λ_{abs} (nm)	*f*	Transition dipole moment (*D*)		
						X	*Y*	*Z*
IFBTP								
$S_0 \rightarrow S_1$	369.42	1.6029	HOMO→LUMO(0.65)	355.2	1.94103	−12.08	0.46	0.16
$S_0 \rightarrow S_2$	328.84	0.0296	HOMO-1→LUMO(0.61)	318.7	0.12357	2.87	−0.01	0.30
$S_0 \rightarrow S_3$	312.32	0.3384	HOMO→LUMO+1(0.60)	306.7	0.01195	0.86	0.15	0.04
$S_0 \rightarrow S_4$	307.10	0.0054	HOMO-2→LUMO(0.54) HOMO→LUMO+2(0.30)	300.0	0.01637	−0.76	−0.68	0.00
$S_0 \rightarrow S_5$	295.43	0.0142	HOMO→LUMO+3(0.55) HOMO-5→LUMO(0.21)	290.1	0.06008	−1.45	1.25	0.03
$(IFBTP)_2$								
$S_0 \rightarrow S_1$	412.44	3.2634	HOMO→LUMO(0.66)	370.0	4.61654	−19.04	0.06	0.20
$S_0 \rightarrow S_2$	381.14	0.3922	HOMO-1→LUMO(0.66)	344.5	0.04840	−1.70	0.70	−0.36
$S_0 \rightarrow S_3$	369.37	0.0313	HOMO→LUMO+1(0.63)	321.5	0.27554	−4.30	0.36	0.40
$S_0 \rightarrow S_4$	354.30	0.8340	HOMO-1→LUMO+1(0.62)	299.4	0.03171	1.38	−0.23	−0.18
$S_0 \rightarrow S_5$	346.04	0.0495	HOMO-2→LUMO(0.53) HOMO→LUMO+2(0.36)	291.6	0.14964	2.86	0.64	−0.80
$(IFBTP)_3$								
$S_0 \rightarrow S_1$	423.65	5.0609	HOMO→LUMO(0.61)	374.1	6.78183	−23.21	0.03	0.01
$S_0 \rightarrow S_2$	397.97	0.0142	HOMO-1→LUMO(0.52) HOMO→LUMO+1(0.40)	358.0	0.01834	−0.06	0.88	0.77
$S_0 \rightarrow S_3$	389.60	0.2381	HOMO→LUMO+1(0.50) HOMO-1→LUMO(0.38)	341.0	0.64353	6.73	−0.10	−1.10
$S_0 \rightarrow S_4$	380.16	0.0572	HOMO-2→LUMO(0.65)	324.3	0.00295	−0.24	−0.14	−0.34
$S_0 \rightarrow S_5$	377.46	0.9596	HOMO-1→LUMO+1(0.62)	313.9	0.09723	2.52	−0.26	−0.20
$(IFBTP)_4$								
$S_0 \rightarrow S_1$	425.80	7.1777	HOMO→LUMO(0.56) HOMO-1→LUMO(0.20)	377.1	8.91604	−26.71	−0.17	0.01
$S_0 \rightarrow S_2$	407.37	0.0156	HOMO-1→LUMO(0.46) HOMO→LUMO+1(0.43)	365.6	0.02087	0.26	−1.14	0.49
$S_0 \rightarrow S_3$	391.76	0.4589	HOMO→LUMO+1(0.38) HOMO-1→LUMO(0.36)	353.2	0.83669	−7.79	0.91	1.05
$S_0 \rightarrow S_4$	390.57	0.2951	HOMO-1→LUMO+1(0.47) HOMO-2→LUMO(0.29)	340.6	0.18245	3.43	−0.66	−0.99
$S_0 \rightarrow S_5$	384.10	0.1063	HOMO-2→LUMO(0.55) HOMO-1→LUMO+1(0.25)	327.0	0.17832	−3.51	0.11	0.11
Exp.	435[a]							

[a] The values are measured in thin film.

4. Conclusion

All the oligomers investigated show slightly more twisted structures compared with pristine polyfluorene by the incorporation with bithieno[3,2-*b*:2′3′-*e*]pyridine (BTP) units. All decisive molecular orbitals are delocalized on both subunits of the oligomers. The HOMO possesses an antibonding character between subunits, which may explain the non-planarity observed for these oligomers in their ground state. On the other hand, the LUMO shows bonding character between the two adjacent rings, in agreement with the more planar S_1 excited state. Importantly, the combination of BTP with the fluorine moieties resulted in the reduce LUMO energies and consequently the electron injection was greatly improved. Excitation to the S_1 state corresponds almost exclusively to the promotion of an electron from the HOMO to the LUMO. Accordingly, the energy of the $S_0 \rightarrow S_1$ electronic transition follows the HOMO–LUMO energy gap of each oligomer. The first electronic transition gives rise to largest values of the oscillator strength in each oligomer. The red-shifted in absorption and emission spectra of PIFBTP compared with PFBTP is attributed to an increase of polymer chain planarity and effective conjugation length upon substitution of indenofluorene for fluorene.

Finally, the good agreement between theoretical electronic transitions and experimental spectra seems to indicate that a rational design the tunable light-emitting fluorine derivatives and related polymers is possible and should then contribute to the development of organic light-emitting diodes.

Acknowledgements

This work is supported by the National Nature Science Foundation of China (No. 90101026) and the Key

Laboratory for Supramolecular Structure and Material of Jillin University.

References

[1] Heeger A-J. Angew Chem Int Ed 2001;40:2591.

[2] (a) Pel Q, Yu G, Zang C, Yang Y, Heeger AJ. Science 1995;269:1086.
(b) Herold M, Gmeiner J, Schworer M. Acta Polym 1994;451:392.

[3] Spangler CW. J Mater Chem 1999;9:2013.

[4] Lovinger AJ, Rothverg LJ. J Mater Res 1996;11:1581.

[5] Forrest SR. Chem Rev 1997;97:1793.

[6] Beaupré S, Leclerc M. Adv Funct Mater 2002;12:192.

[7] Lévesque L, Donat-bouillud A, Tao Y, D'Iorio M, Beaupré S, Blondin P, et al. Synth Met 2001;122:79.

[8] Lee JI, Klaerner G, Davey MH, Miller RD. Synth Met 1999;102:1087.

[9] Charas A, Barbagallo N, Morgado J, Alcacer L. Synth Met 2001;122:23.

[10] Weiss H, Steiger S, Jungling S, Yakimansky AV, Muller A-H-E. Macromolecules 2003;36:3374–9.

[11] Mushrush M, Facchetti A, Lefenfeld M, Katz HE, Marks TJ. J Am Chem Soc 2003;125:9414–23.

[12] Brédas JL, Silbey R, Boudreaux DS, Chance RR. J Am Chem Soc 1983;105:6555–9.

[13] Tavan P, Schulten K. J Chem Phys 1986;85:6602–9.

[14] Beljonne D, Shuai Z, Cornil J, dos Santos DA, Bredas JL. J Chem Phys 1999;32:267–76.

[15] Lahti PM, Obrzut J, Karasz FE. Macromolecules 1987;20:2023–6.

[16] Seixas de Meloa J, Burrows HD, Svensson M, Andersson MR, Monkman AP. J Chem Phys 2003;118:1550.

[17] Scheinert S, Schliefke W. Synth Met 2003;139:501–9.

[18] Salzner U, Lagowski JB, Pickup PG, Poirier RA. Synth Met 1998;96:177–89.

[19] Hutchison G-R, Ratner M-A, Marks T-J. J Phys Chem B 2005;109:3126–38.

[20] Zhang J-P, Frenking G. J Phys Chem A 2004;108:10296–301.

[21] Kwon O, McKee M-L. J Phys Chem A 2000;104:7106–12.

[22] Daminlli G, Widany J, Carlo A-D, Lugli P. J Chem Phys 2001;115:4919–23.

[23] Jespersen K-G, Beenken W-J-D, Zaushitsyn Y, Yartsev A, Andersson M, Pullerits T, et al. J Chem Phys 2004;121:12613–7.

[24] Briére J-F, Côté M. J Phys Chem B 2004;108:3123–9.

[25] Grozema F-C, van Duijnen P-T, Siebbeles L-D-A, Goossens A, de Leeuw A-W. J Phys Chem B 2004;108:16139–46.

[26] Grozema FC, Candeias LP, Swart M, van Duijnen P-T, Wildeman J, Hadziioanou G, et al. J Chem Phys 2002;117:11366–78.

[27] Fratiloiu S, Grozema F-C, Siebbeles L-D-A. J Phys Chem B 2005;109:5644–52.

[28] Zhan CG, Nichols J-A, Dixon D-A. J Phys Chem A 2003;107:4184–95.

[29] Sonar P, Zhang J, Grimsdale AC, Mullen K, Surin M, Lazzaroni R, et al. Macromolecules 2004;37:709–15.

[30] Brébdas J-L, Silbey R, Boudreaux D-S, Chance R-R. J Am Chem Soc 1983;105:6555–9.

[31] Ford W-K, Duke C-B, Paton A. J Chem Phys 1982;77(9):4564–72.

[32] Klaerner G, Miller RD. Macromolecules 1998;31:2007–9.

[33] Brébdas J-L, Chance R-R, Silbey R. Phys Rev B 1982;26:5843–54.

[34] Ma J, Li S-H, Jiang Y-S. Macromolecules 2002;35:1109–15.

[35] Zhang G-L, Ma J, Jiang Y-S. Macromolecules 2003;36:2130–40.

[36] Cao H, Ma J, Zhang G-L, Jiang Y-S. Macromolecules 2005;38:1123–30.

[37] Zhou X, Ren A-M, Feng J-K. Polymer 2004;7747–57.

[38] Wang JF, Feng JK, Ren AM, Liu XD, Ma YG, Lu P, et al. Macromolecules 2004;37:3451.

[39] (a) Yang L, Ren AM, Feng JK, Liu XD, Ma YG, Zhang HX. Inorg Chem 2004;43:5961.
(b) Yang L, Ren AM, Feng JK, Ma YG, Zhang M, Liu XD, et al. J Phys Chem 2004;108:6797.

[40] Frisch MJ, Trucks GW, Schlegel HB, Scuseria GE, Robb MA, Cheeseman JR, Montgomery JA Jr, Vreven T, Kudin KN, Burant JC, Millam JM, Iyengar SS, Tomasi J, Barone V, Mennucci B, Cossi M, Scalmani G, Rega N, Petersson GA, Nakatsuji H, Hada M, Ehara M, Toyota K, Fukuda R, Hasegawa J, Ishida M, Nakajima T, Honda Y, Kitao O, Nakai H, Klene M, Li X, Knox JE, Hratchian HP, Cross JB, Adamo C, Jaramillo J, Gomperts R, Stratmann RE, Yazyev O, Austin AJ, Cammi R, Pomelli C, Ochterski JW, Ayala PY, Morokuma K, Voth GA, Salvador P, Dannenberg JJ, Zakrzewski VG, Dapprich S, Daniels AD, Strain MC, Farkas O, Malick DK, Rabuck AD, Raghavachari K, Foresman JB, Ortiz JV, Cui Q, Baboul AG, Clifford S, Cioslowski J, Stefanov BB, Liu G, Liashenko A, Piskorz P, Komaromi I, Martin RL, Fox DJ, Keith T, Al-Laham MA, Peng CY, Nanayakkara A, Challacombe M, Gill PMW, Johnson B, Chen W, Wong MW, Gonzalez C, Pople JA. Gaussian 03, Revision B.04, Gaussian, Inc., Pittsburgh PA; 2003.

[41] Foresman JB, Head-Gordon M, Pople JA. J Phys Chem 1992;96:135.

[42] Belletete M, Beaupre S, Bouchard J, Blondin P, Leclerc M, Durocher G. J Phys Chem B 2000;104:9118–25.

[43] De Oliveira MA, Duarte HA, Pernaut J-M, De Almeida WB. J Phys Chem A 2000;104:8256–62.

[44] Cornil J, Gueli I, Dkhissi A, Sancho-Garcia J-C, Hennebicq E, Calbert J-P, et al. Phys Rev B 2003;118:6615–23.

[45] Hsu C, Hirata S, Martin H. J Phys Chem A 2001;105:451–8.

[46] Cai A, Sendt K, Reimers J-R. J Chem Phys 2002;117:5543–9.

[47] Tozer D-J, Handy N-C. J Chem Phys 1998;109:10180.

[48] Casida M-E, Jamorski C, Casida K-C, Salabub D-R. J Chem Phys 1998;108:4439.

[49] Puschning PA, Mbrosch-Draxl C, Heimel G, Zojer E, Resel R, Leising G, et al. Synth Met 2001;116:327.

[50] Eaton VJ, Steele D. J Chem Soc, Faraday Trans 2 1973;2:1601.

[51] Almenningen A, Bastiansen O, Fernholt L, Cyvin B, Cyvin S, Samdal S. J Mol Struct 1985;128:59.

[52] Lin B-C, Cheng C-P, Michael Lao Z-P. J Phys Chem A 2003;107:5241–51.

[53] Curioni A, Boero M, Andreoni W. Chem Phys Lett 1998;294:263–71.

[54] Wang I, Estelle BA, Olivier S, Alain I, Baldeck PL. J Opt A: Pure Appl Opt 2002;4:S258–S60.

[55] Grimme S, Parac M. Chem Phys Chem 2003;3:292.

[56] Ortiz RP, Delgado MCR, Casado J, Hernández V, Kim OK, Woo HY, et al. J Am Chem Soc 2004;126:13363.